

Cambridge University Press

978-1-107-01258-5 - Quantum Dots: Optics, Electron Transport and Future Applications

Edited by Alexander Tartakovskii

Excerpt

[More information](#)

Part I

Nanostructure design and structural properties of
epitaxially grown quantum dots and nanowires

Cambridge University Press

978-1-107-01258-5 - Quantum Dots: Optics, Electron Transport and Future Applications

Edited by Alexander Tartakovskii

Excerpt

[More information](#)

1

Growth of III–V semiconductor quantum dots

C. Schneider, S. Höfling and A. Forchel

1.1 Introduction

The advanced growth of semiconductor quantum dots (QDs) with high optical quality is one key to realizing novel devices in various research disciplines related to modern semiconductor technologies. Despite recent progress in the top-down lithographic fabrication of single semiconductor QD-like emitters [43], bottom-up fabrication methods are commonly applied for the realization of high quality light emitting QDs [7]. The exploitation of high-density QD arrays as an active material in laser diodes [17] and vertical cavity surface emitting lasers (VCSEL) resulted in a new class of devices featuring lower lasing thresholds and improved device performance (such as temperature stability) in comparison to devices with higher dimensional gain [2, 3].

Spintronics and quantum information processing are intensively studied fields in order to provide complementary or entirely novel routes to a future information technology [12, 5]. Single self-assembled quantum dots (QDs) grown in low-density arrays are promising candidates for realizing functional building blocks in these research fields as they allow to confine single charge carriers or spin carriers while providing a solid-state platform capable of electrical injection or manipulation. Extensive research has resulted in the realization of various devices relying on few or single QDs, for instance quantum light emitters such as single photon sources [23, 36], sources of pairs of entangled photons [1, 45], and few-to single-QD lasers [38]. Moreover, many milestone experiments have been performed with In(Ga)As QDs grown on GaAs, for instance the observation of the Purcell effect [10] or reaching the strong QD exciton–photon coupling regime [26], demonstration of the indistinguishability of photons emitted by a QD [29], or complete control of a single spin by ultrafast optical pulses [25]. A desirable feature of these single QDs is a very high optical quality.

Material engineering and epitaxial growth techniques on GaN [15], GaAs and InP substrates have paved the way to realize optically active QD structures and QD-based devices in a wide spectral range throughout almost the entire visible spectral range up to emission wavelength in the important telecommunication bands at 1.3 μm and 1.55 μm .

In this chapter we concentrate on QD growth on GaAs. Please note that site-selected QD growth on InP substrate for long-wavelength applications (e.g. [8]) will be addressed in

chapter 19 of this book. One main focus of the present summarized work lies on the growth of low-density QD arrays emitting in various wavelength regimes. In order to scalably fabricate single QD-relying devices, it is of the utmost interest to achieve a high degree of control over the position of single QDs in dilute arrays with periods exceeding the device dimensions [32, 9]. Therefore we will summarize various complementary attempts to realize site-controlled QD arrays on an GaAs substrate, suitable for device integration.

1.2 Properties of semiconductor quantum dots

1.2.1 Growth of Stranski–Krastanov and site-controlled quantum dots

In this section, we will briefly describe the processes involved during the growth of QDs in the Stranski–Krastanov (SK) mode as well as on patterned substrates. During the heteroepitaxial growth of various semiconductor materials with slightly differing lattice constants, such as InAs on GaAs (7% lattice mismatch), the grown material at first usually adapts the in-plane lattice constant (Fig. 1.1a) of the substrate and is grown pseudomorphically. During this growth process, strain accumulates in the layer system (Fig. 1.1b). After a certain layer thickness is exceeded the strain in the coherently strained layer eventually relaxes partially, resulting in the formation of islands on the surface in order to minimize the total layer energy (Fig. 1.1c). By applying the right growth conditions these islands can be free of crystal defects and their dimensions can be comparable with the exciton Bohr radius in the semiconductor. This SK growth mode was observed in a number of III–V semiconductor systems, including (Al,Ga)InAs on (Al)GaAs, (Ga)InP on Ga(In)P or InAs on (Ga)InP. The morphology of the QDs can be widely tailored by altering the strain in the material system, e.g. via the composition in ternary QDs, as will be described in Section 1.3.1. Furthermore, the surface migration during QD deposition is another important tool for actively manipulating the morphology and the density of the QDs. In this context, the substrate temperature and the ratio of group III–V elements during sample growth have a wide impact on these properties.

The strain-driven nucleation of QDs in the SK mode is self-organized and hence the QDs are usually randomly distributed over the sample. In order to obtain a higher degree of control over the QD positions, several concepts were developed to grow ordered arrays of QDs. The basic mechanism in most of these concepts is to obtain control over the

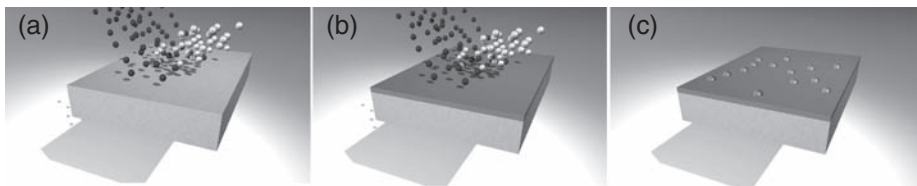


Figure 1.1 Growth of QDs in the Stranski–Krastanov mode. (a) Deposition of the QD material on a GaAs surface. (b) Evolution of a strained wetting layer. (c) Nucleation of coherent islands.

surface binding energies or surface migration length of the adatoms. These adatoms preferentially nucleate at positions with a lower chemical surface potential. Hence, the nucleation of QDs can be actively manipulated by artificially defining crystal edges, nanopits or pyramids on a crystal surface by lithographic techniques before growing the QDs. We refer the reader to reference [31] for a detailed introduction into site-selected QD growth techniques.

1.2.2 Electronic and spectral properties of quantum dots

The unique characteristics of semiconductor QDs originate in pronounced quantization effects and the discrete density of states (DOS) of the quasi zero-dimensional structures. Like single atoms, QDs exhibit a shell structure and the occupation of these shells follows Pauli's principle. A feature that is unique to these 'artificial atoms' is the concept of excitons. These are quasi particles composed of a negatively charged electron in the conduction band and a positively charged hole in the valence band of the semiconductor. Owing to attractive coulomb forces, the electron and the hole form an exciton which can be spatially confined inside the QD due to the energetic band offsets in the heterostructure. The delocalization area of the exciton in bulk material is often described by the exciton Bohr radius, $a = \frac{4\pi\epsilon_0\epsilon_r\hbar^2}{\mu e^2}$, which is usually comparable to the extension of the QD.

The calculated first two single particle eigenenergies of a truncated pyramidal Ga_{0.5}In_{0.5}As QD in the electron and the hole band are shown in Fig. 1.2a, revealing the quantization of the energy levels. Because of the larger effective mass, the lowest energy state of such a system is formed with the heavy hole (HH) in the valence band. In an ideal system, only the indicated transitions between 1s-1HH and 2s-2HH are allowed due to the symmetry of the wavefunctions. This atom-like shell structure can be observed in single QD studies as described in the experimental part of this chapter. Owing to the self-organized fabrication process of the QDs, inhomogeneities in size and material

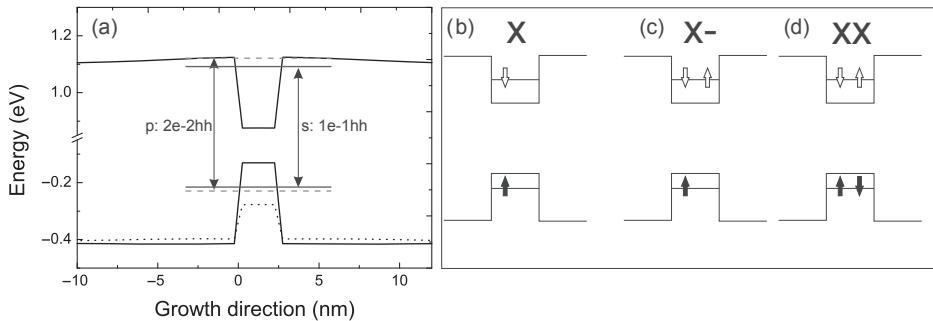


Figure 1.2 (a) Calculated energy structure of a truncated pyramidal QD. Discrete energy levels are formed in the electron and hole band, leading to an atom-like shell structure. (b)–(d) Selected charge and spin configurations in the s-shell, often referred to as exciton X, trion X[−] (X⁺ analogous) and biexciton (XX).

composition between different QDs are almost unavoidable. These fluctuations directly manifest themselves in an energy spread of the emission lines up to several tens of millielectronvolts of the QDs, e.g. in a photoluminescence (PL) experiment. Therefore, the inhomogeneous broadening of the ensemble PL signal recorded from a large number of QDs gives direct information about the homogeneity of the QDs. In the light of the exploitation of QDs as a gain material in laser structures, the inhomogeneous ensemble broadening is a figure of merit, since a narrow emission spectrum can lead to a higher material gain and hence improved device characteristics. Since the occupation of the QD shells follows Pauli's principle, the ground state of the QD can be occupied by only a maximum of two electrons and two holes of opposite spin. This configuration is often referred to as the biexciton (see Fig. 1.2d), of which the emission energy is usually shifted by coulomb and exchange interaction with respect to the exciton emission energy. Configurations with a single unpaired spin carrier are mainly referred to as trions or charged excitons. This zoo of excitonic complexes is indicated in Fig. 1.2b–d. If more charges are filled into the QD, higher shells are occupied with emission bands at notably higher energies.

1.3 Epitaxial growth of quantum dots on GaAs substrates

In this section, we summarize the basic morphologic and spectral characteristics of QDs grown on GaAs substrate. The influence of material strain and surface migration length on the QD shape and density are addressed exemplarily for the (Ga)InAs/GaAs QD model system. We will furthermore discuss ensemble and single QD emission properties of these QDs. Finally, approaches for achieving high control over the QD positions are reviewed.

1.3.1 Influence of material strain on the formation of GaInAs quantum dots

Since material strain is the driving mechanism in the SK growth mode, it has large impact on the QD morphology and therefore on the optical properties. In order to illustrate this, we compare QD samples all containing GaInAs/GaAs QDs with nominal indium contents of 60%, 45%, and 30%. For the $\text{Ga}_{0.4}\text{In}_{0.6}\text{As}$ QDs, 1.4 nm of material was deposited at a surface temperature of 470 °C by molecular beam epitaxy [13]. QDs with an indium content of 45% and 30% were realized by depositing 2.1 nm and 4.5 nm respectively, at 510 °C. The amount of deposited GaInAs material is increased for the QD samples with lower indium content taking account of the larger critical thickness [34].

Figure 1.3 shows scanning electron microscopy (SEM) images of uncapped QD structures. In order to enhance the image contrast, the surfaces were tilted by 70°. The QDs with an indium content of 60% have diameters between 10 nm and 15 nm, and a rather high QD density of about $1\text{--}2 \cdot 10^{11} \frac{1}{\text{cm}^2}$. For single QD applications, the dot density should be much lower. In order to realize dilute arrays of QDs, the substrate temperature for the 45% and 30% In QDs was increased to 510 °C to enhance the migration length [20]. As a result, the QDs with 45% In content are lens-shaped structures with increased diameter

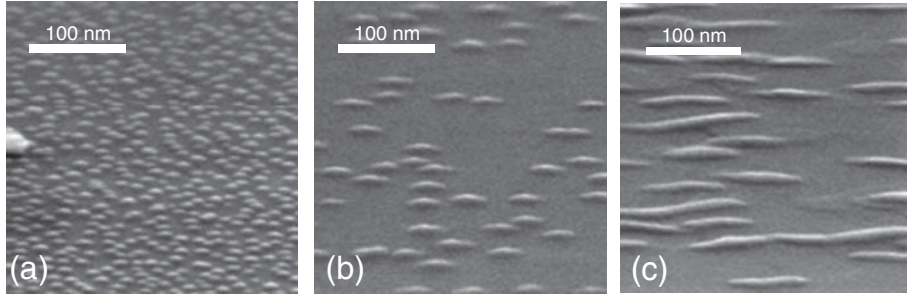


Figure 1.3 Surface SEM images of three uncapped QD samples with different indium contents of (a) 60%, (b) 45% and (c) 30%.

of 20–25 nm and a notably reduced QD density of about $1\text{--}2 \cdot 10^{10} \frac{1}{\text{cm}^2}$. To increase the single QD's volume, the strain of the QD structures was reduced once more by decreasing the In content to 30%. Because of the low-strain condition, the island growth is mainly initiated by crystal steps on the surface. This induces the formation of elongated dot structures in Fig. 1.3c which are preferentially orientated along the $[0\bar{1}1]$ direction with typical lengths of 50–100 nm and widths of about 30 nm as can be extracted from the uncapped structures. The combination of low-density QD growth, the material-related short emission wavelength below 950 nm and large QD volumes resulting in enhanced exciton dipole moments makes these QDs interesting for the study of light–matter coupling.

1.3.2 Quarternary AlGaInAs quantum dots with tailored morphology and emission wavelength

As described above, the morphology of SK QDs is strongly related to the material strain and also to the surface temperature during deposition. The emission wavelength of these QDs cannot be independently tailored in these systems but depend strongly on the material alloy, the QD size and the strain in the islands. In order to independently tailor QD morphology and emission wavelength of the QDs, the growth of quarternary AlGaInAs QDs was established, because the strain mainly depends on the indium fraction while the QD bandgap can be conveniently adjusted by the aluminum vs. gallium fraction [30].

First, we want to clarify the influence of the aluminum content on the QD morphology by studying uncapped QDs on top of an $\text{Al}_{0.34}\text{Ga}_{0.66}\text{As}$ surface. The pronounced dependence of the QD density and the lateral size on the Al and the In content is summarized in Fig. 1.4a, and b for two sample series with a different indium content of 47% and 60%, and varying aluminum contents. It can be clearly seen that, for both indium contents, the QD surface density increases and the average QD diameter decreases with increasing aluminum content.

The fact that the QD density and the average QD size show similar behavior for both moderate and high indium content indicate that these quantities are mainly determined

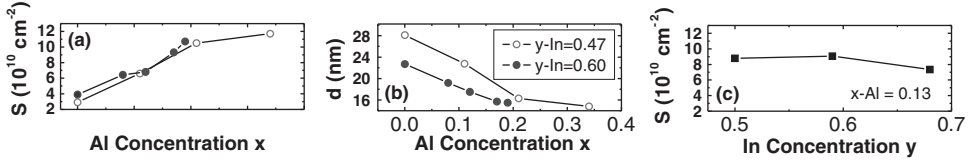


Figure 1.4 (a) QD surface density S and (b) average lateral QD size d for $\text{Al}_x\text{Ga}_{1-x-y}\text{In}_y\text{As}$ QDs with two different indium contents ($y = 0.47$ and 0.60) as a function of aluminum content x . (c) QD surface density S of $\text{Al}_{0.13}\text{Ga}_{0.87-y}\text{In}_y\text{As}$ QDs as a function of indium content y .

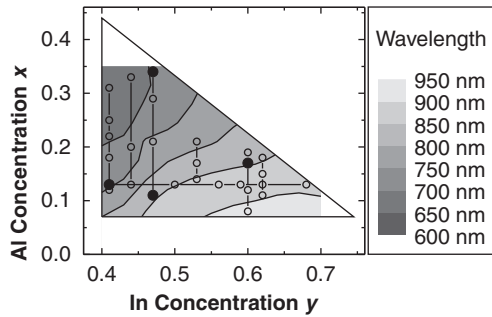


Figure 1.5 QD emission wavelength plotted vs. indium and aluminum content. The emission wavelength is encoded in the gray scale of the graph.

by the aluminum content. Figure 1.4c, which shows the dependence of the QD surface density S on the indium content for a constant aluminum content of $x = 0.13$ supports this conclusion, since only minor changes in the QD density could be observed for indium contents between 50% and 68%. We will now focus on the effect of the aluminum content in the QDs on the emission wavelength of the QD ensembles.

In order to provide electronic confinement in the QDs, the structures were integrated in an $\text{Al}_{0.34}\text{Ga}_{0.66}\text{As}$ matrix for spectroscopic investigations. Figure 1.5 shows an interpolated contour plot of the PL wavelengths (at $T = 8 \text{ K}$) of 32 QD samples examined as a function of the indium and aluminum contents. Some data points of the systematically acquired grid used to create the figure are indicated in the plot. Apparently the wavelength of the quaternary AlGaInAs QDs can be widely tuned in a range between 660 nm and 940 nm by varying the aluminum and indium contents. Furthermore, it is possible to identify many different QD compositions that would result in the same emission wavelength. Along these iso-wavelength lines it is possible to choose between QD ensembles with morphological properties best suited for the intended application [30].

1.3.3 Morphologic and optical properties of low density InAs quantum dots

The growth of QD arrays with dilute areal densities is a pre-requisite for exploiting the unique properties of the nanostructures in devices relying on single QDs. Typically, the

structures that are used in these applications have sizes of several hundred nanometers up to several microns. Therefore it is highly desirable to integrate QD arrays with densities well below $1 \cdot 10^{10} \frac{1}{\text{cm}^2}$ in order to facilitate the observation of single QD related effects. Considering adsorbant binding energies and the ability to migrate on a GaAs surface, the most promising candidates to realize very dilute arrays of QDs is the binary InAs material system. During the QD deposition, the morphology of the structures is mainly determined by the surface migration. Hence, a more detailed investigation of the influence of the surface temperature and deposited amount of material is essential. Since the growth rate also has a strong influence on the QD morphology, the surface migration length during QD growth was enhanced by lowering the InAs growth down to $0.008 \frac{\text{nm}}{\text{second}}$. The investigated QD samples were realized by the deposition of 1 nm InAs at substrate temperatures of 510 °C, 513 °C and 517 °C during QD deposition. Figures 1.6a–c show SEM images of the according uncapped QDs. The QD density reduces from a value of $2.34 \cdot 10^{10} \frac{1}{\text{cm}^2}$ for 510 °C down to a value of $5.23 \cdot 10^9 \frac{1}{\text{cm}^2}$ at 517 °C. Additionally, the lateral extension of the QD increases from 32.7 nm to 39.5 nm when increasing the surface temperature (see Fig. 1.6d).

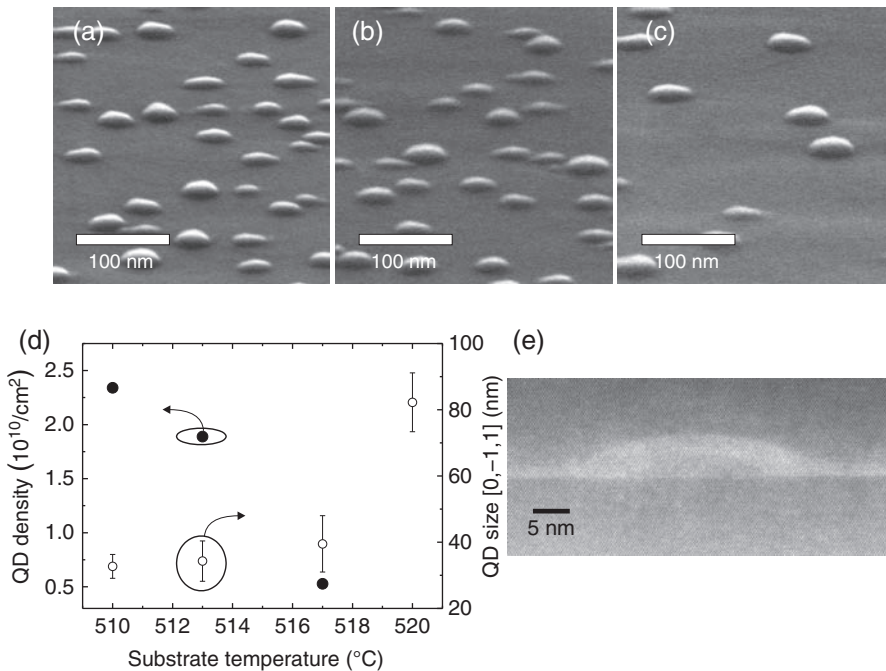


Figure 1.6 SEM images of uncapped InAs QDs grown at substrate temperatures of (a) 510 °C, (b) 513 °C and (c) 517 °C. (d) The QD density decreases with increasing substrate temperature, accompanied by larger lateral dimensions. (e) Scanning transmission electron micrograph of a single InAs QD overgrown by GaAs. The QD features a smooth lens shape with an approximate height of 5 nm on top of a thin wetting layer.

Because it is known that the morphology of QDs can be strongly affected by the overgrowth with GaAs material, additional scanning transmission electron micrographs (STEM) were carried out on buried InAs QDs with a low area density (Fig. 1.6e). The cross-sectional image of the buried QD again reveals the lens shape of the QD, with a QD height of about 5 nm and a baselength of 30 nm on top of a thin wetting layer.

Besides tailoring the morphology of the QDs, a high degree of emission control of the QDs is crucial in order to achieve complex devices and building blocks for QD-based quantum information technology.

- **Single QD-based efficient single photon sources.** In order to improve the efficiency of the single photon extraction process, QDs are often integrated into optical microcavities. On spectral resonance, the QD emission rate can be significantly enhanced via the Purcell effect, and furthermore the emission can be directed into a collimation lens. In order to realize resonance between the QD and the cavity, the emission wavelength of the QDs needs to be matched to the resonance frequency of the device. This implies the necessity of accurately controlling the emission wavelength of the QDs during growth. Furthermore, since the sensitivity of commercial silicon-based single-photon detectors continuously increases in the spectral range from 1 μm down to wavelengths around 600 nm, the QD emission wavelength should be chosen appropriately. Additionally, it is also interesting to realize QD-based single-photon emitters in the spectral range of the dispersion and absorption minima of optical fibers, namely at wavelengths of 1.3 μm and 1.55 μm [40]. Furthermore, in order to enhance the emission rate of the QDs themselves, it's promising to circumvent long-living dark states in the QDs, for instance by doping the QDs to preferentially create charged excitons [39].
- **Polarization entangled photon pairs.** Utilizing the cascaded emission from the XX and X states of a single QD, polarization-entangled photons can be generated. One pre-requisite is the suppression of the fine-structure splitting of these emission features (within the homogeneous broadening of the emission lines), caused by structural asymmetries of the nanostructures [36].
- **Spin-Qubits.** Single spin carriers (electrons or holes) which are spatially confined in a QD are potential candidates for stationary quantum bits (Qubit), and therefore the basic building blocks for quantum computers [18]. Owing to the localization of the spin carriers in InAs QDs effects of spin dephasing via phonon coupling and therefore the loss of information can be notably suppressed. Furthermore, resonant optical pumping of the trion states in an external magnetic field can facilitate the initialization of the Qubit on a timescale of a few nanoseconds [25] and a ratio of up to 10^5 gate operations per dephasing time has already been demonstrated. For these kinds of experiments, the charged trion state of the QDs especially needs to be controlled.

Since the emission properties of the QDs (especially the emission wavelength) strongly depend on the morphology and alloy [19, 30], it can be challenging to optimize the QD morphology and emission properties independently via the growth conditions and material